Journal of Materials Chemistry C

Accepted Manuscript

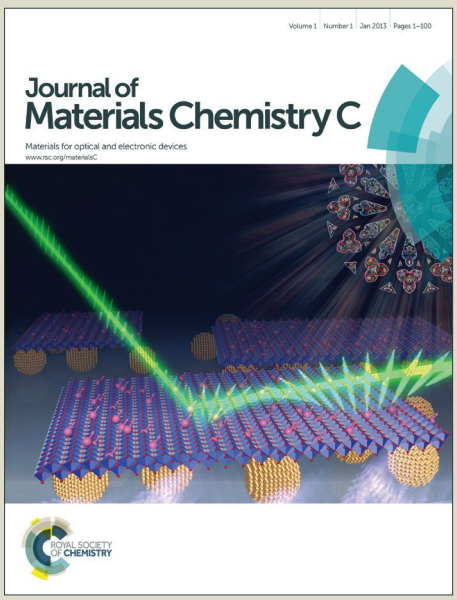

ROYAL SOCIETY OF CHEMISTRY

www.rsc.org/materialsC

Journal Name

COMMUNICATION

A thermally activated delayed blue fluorescence emitter with reversible externally tunable emission

Received 00th January 20xx,
Accepted 00th January 20xx

DOI: 10.1039/x0xx00000x

www.rsc.org/

Pachaiyappan Rajamalli,[a] Natarajan Senthilkumar,[a] Parthasarathy Gandeepan,[a] Chen-Zheng Ren-Wu,[b] Hao-Wu Lin[b] and Chien-Hong Cheng*[a]

A thermally activated delayed fluorescence (TADF) material containing two *meta* carbazolyl groups on the phenyl ring of benzoyl-4-pyridine moiety was prepared and its luminescence shows colour change from blue to green by external stimuli. The organic-blue-light-emitting device using this TADF dopant provided a high external quantum efficiency of 18.4%.

Tuning and controlling the solid-state emission of π-conjugated organic materials constitute an attractive area of research for both fundamental interest and as a key component of many advanced applications in the fields of lighting, data storage, security inks, sensors, and re-writable media.[1] Re-writable materials would significantly reduce printer paper usage and save millions of trees.[2] The promising features of these materials has attracted significant attention and a number of studies have been reported on vapo, mechano/piezo, and acido-responsive π-conjugated organic fluorescent materials.[3] Nevertheless, materials with easy access, multiple applications, and high-contrast reversible-switching luminescence remain rare. Very recently, thermally activated delayed fluorescence (TADF) materials have attracted much attention due to their wide applicability in areas such as display, lighting, and biotechnology.[4] Mainly, TADF materials shed light on OLED development due to 100% internal quantum efficiency can be achieved by harvesting both singlet and triplet excitons by reverse intersystem crossing (RISC) from the lowest triplet (T_1) state to lowest singlet (S_1) state.[5] A very small energy gap between the S_1 and T_1 states (ΔE_{ST}) is required to activate TADF because the rate of RISC is inversely proportional to the exponent of ΔE_{ST}.[6] Based on this required criteria, TADF compounds have been designed and synthesized.[7] However, the developed blue TADF emitter to achieve efficient OLEDs are limited. Therefore, there is a strong demand for the development of high efficiency blue TADF OLEDs to replace the expensive and less stable blue phosphorescent materials. Although conventional fluorescent materials and metal complexes have been reported with mechanoluminescent properties, TADF materials with reversible tunable emission have not been reported so far. Hence, the development of new organic TADF materials that can be applied in efficient organic light-emitting diodes (OLEDs) and also exhibit solid state enhanced emission and mechanoluminescence is of great importance both scientifically and practically.

Here, we have synthesized a benzoylpyridine-based blue TADF emitter, (3,5-di(9*H*-carbazol-9-yl)phenyl)(pyridin-4-yl)methanone (*m*DCBP) (Scheme 1) which exhibits highly enhanced solid state emission compared to the solution emission. Simultaneously, this molecule exhibits reversible switchable emission via alternating applied mechanical force and solvent fuming. This is a development over most reported mechanoluminescence (ML) materials that exhibited weak solid-state emission. *m*DCBP also exhibited a very small ΔE_{ST} of 0.06 eV, with small spatial overlap between highest occupied molecular orbital (HOMO) and lowest unoccupied molecular orbital (LUMO). Transient PL measurements revealed the TADF property clearly. The use of this TADF emitter for blue and green OLEDs gave high external quantum efficiency (EQE) of 18.4% and 14.7%, respectively.

The *m*DCBP can be easily synthesized in two steps as shown in Scheme 1, with the detailed synthetic procedure given in the Supporting Information. The compound was purified by temperature-gradient vacuum sublimation and characterized by ^{1}H and ^{13}C NMR, and high-resolution mass spectrometry. Further, the structure was confirmed by single-crystal X-ray analysis. As depicted in Fig. 1a, the HOMO of *m*DCBP is distributed over one of the carbazolyl groups, with the HOMO+1 localized over the other carbazolyl group (Fig. S1). Conversely,

[a]*Department of Chemistry, National Tsing Hua University, Hsinchu 30013, Taiwan. E-mail: chcheng@mx.nthu.edu.tw*
[b]*Department of Materials Science and Engineering, National Tsing Hua University, Hsinchu 30013, Taiwan*
Electronic Supplementary Information (ESI) available: General information, computational details, UV-Vis, Pl, CV, TGA, DSC, current density and luminance vs driving voltage and current efficiency vs luminance . See DOI: 10.1039/x0xx00000x

time-dependent DFT (TDDFT) revealed that the LUMO is mostly localized on the benzoyl pyridine (BP) core. There is only a small overlap of the HOMO and LUMO at the centre phenyl group. In addition, the calculation showed a small singlet and triplet energy gap (ΔE_{ST}) of 0.15 eV; this value is comparable to reported TADF emitters.[5]

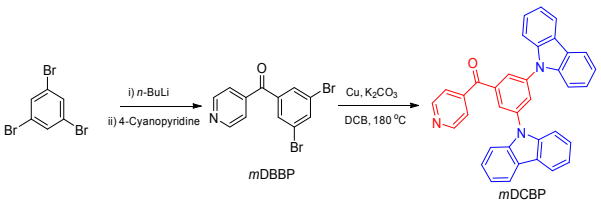

Scheme 1 Synthesis of *m*DCBP.

The absorption and emission spectra of *m*DCBP in various solvents are shown in Fig. 1 and Fig. S2 and are summarized in Table 1. In these solutions *m*DCBP exhibits a broad absorption at 372 nm, attributed to the charge transfer (CT) associated with the electron transfer from the carbazole groups to benzoyl pyridine. No significant change was observed in the absorption spectra in various solvents. Conversely, *m*DCBP displays a significant solvatochromic effect of its fluorescent emission, from deep blue (422 nm) in *n*-hexane to green (536 nm) in dichloromethane (Fig. 1c). The phosphorescent emission spectrum of *m*DCBP, taken at 77 K in toluene (10^{-5} M), is also shown in Fig. 1b; the observed peaks were centred at 467 nm. The triplet energy levels were calculated to be 2.94 eV from the onset of the phosphorescence spectrum. The singlet energy gaps calculated from the onset of fluorescence spectrum was 3.0 eV as summarized in Table 1. The ΔE_{ST} was estimated to be 0.06 eV based on the onset of emission in the fluorescence and phosphorescence spectra; these values are even smaller than that obtained from the TDDFT calculation. The small ΔE_{ST} indicate that this molecule plausibly possess TADF properties with efficient up-conversion from T_1 to S_1.

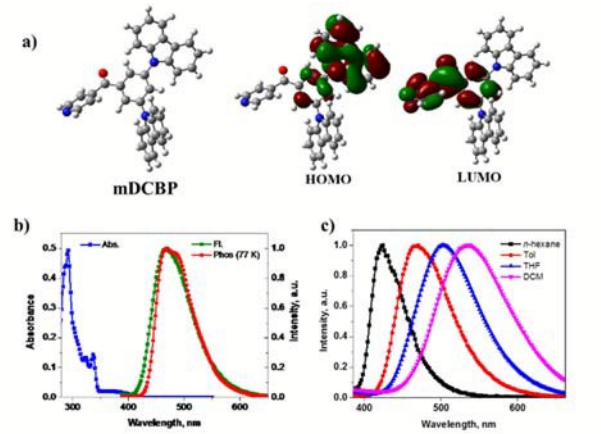

Fig. 1 a) Optimized structure and calculated HOMO and LUMO of *m*DCBP; b) Absorption (Abs.) and emission (Fl.) spectra of *m*DCBP (10^{-5} M) were measured at room temperature in toluene and the phosphorescence (phos.) spectrum measured at 77 K; c) emission spectra of *m*DCBP (10^{-5} M) in various solvents at room temperature.

The electrochemical properties of *m*DCBP were investigated by cyclic voltammetry (Fig. S3). From the onset of oxidation potential (Fig. S3), the HOMO level was calculated to be 5.72 eV. The LUMO energy level as estimated from HOMO - E_S is 2.72 eV. In deoxygenated benzene a quantum yield of 6% is found; this decreases to 1.7% in the presence of oxygen. This efficiency decrease in the presence of oxygen also supports assignment of TADF[5a] and suggests that the T_1 states are readily quenched by the oxygen triplet ground state.

In addition, an absolute photoluminescence quantum yield was measured in a co-doped film (DPEPO:*m*DCBP (10%)) to be 90%, which is much higher than in solution. This arises from the absence of intramolecular rotation and collisional quenching in the solid state. Notably, the PL quantum yield decreased from 90% under nitrogen to 73% under oxygen atmosphere revealing the formation of triplet via intersystem crossing in the DPEPO:*m*DCBP thin film during the PL process (vide supra). It is known that a triplet excited state can be readily quenching by oxygen.[5a] The transient PL decay characteristic of the material in toluene was measured under vacuum and is shown in Fig. 2. As shown in Fig. 2, transient decay curves can be divided into two components. The first represents the prompt emission decay curve from S_1 to the singlet ground state (S_0); the emission lifetime (τ) was calculated from the intensity vs time plot to be 6.2 ns. The second component represents a delayed emission component with τ = 0.2 µs; the delayed emission may be rationalized as the thermal up-conversion of T_1 to S_1, followed by fluorescent relaxation from S_1 to the S_0. The short excited-state lifetime of this molecule is lower than the highly emissive phosphorescent iridium complexes.[8] This is an important feature of TADF emitters that realizes high quantum efficiency and reduces non-radiative decay.

The transient Pl characteristics were measured at temperature from 200-300 K and shown in Figure S4a. The delayed emission component gradually increases with increasing temperature from 200 K to 300 K, due to RISC is increased when the temperature increased. The results further support that *m*DCBP is TADF material.[7c] The delayed emission component intensity at 300 K slightly decreased compared to that at 250 K, due to the fact that the T_1 to S_0 non-radiative decay increased at higher temperature. The prompt and decay PL spectra of the co-doped film are shown in Figure S4b. The delayed PL component can be ascribed to the TADF emission because the prompt and delayed emission spectra coincide with each other. The thermal properties of these emitters were

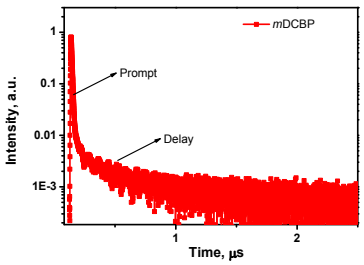

Fig. 2 Transient PL trace of *m*DCBP.

Table 1. Physical properties of *m*DCBP

Compound	λ_{abs} (nm)[a]	λ_{em} (nm)[a]	λ_{em} (nm)[b]	T_g (°C)[c]	T_d (°C)[d]	HOMO (eV)[e]	LUMO (eV)[f]	E_g (eV)[g]	E_T (eV)[h]	Thin film (%)[i]
*m*DCBP	334, 372	467	467	105	394	5.72	2.72	3.0	2.94	90

[a]Measured in toluene (1×10^{-5} M) at room temperature. [b]Phosphorescence measured in toluene (1×10^{-5} M) at 77 K. [c]Obtained from DSC measurements. [d]Obtained from TGA measurement. [e]Measured from the oxidation potential in 10^{-3} M DCM solution by cyclic voltammetry. [f]Measured from HOMO - E_g. [g]Estimated from the onset of fluorescence spectrum. [h]Estimated from the onset of phosphorescence spectrum. [i]Absolute total PL quantum yield evaluated for 10 wt% *m*DCBP doped in DPEPO film using an integrating sphere.

investigated by thermogravimetric analysis (TGA) and differential scanning calorimetry (DSC) under a nitrogen atmosphere; results are shown in Fig. S5 and S6. The compound possesses very high thermal stability with a decomposition temperature (T_d) of 394 °C and a glass transition temperature (T_g) of 105 °C. This high thermal stability endows high morphological stability in the film.

It is interesting to mention that *m*DCBP exhibits blue emission (460 nm) in the crystalline phase and green emission (510 nm) when in the amorphous glassy form. This tunable emission is shown in Fig. 3. These two different forms were obtained by controlling the cooling rate of the vacuum sublimation process, with slow cooling yielding the crystalline form and fast cooling yielding the glassy form. Further, the crystalline form shows reversible high-contrast piezochromism. As a crystalline sample was ground with a mortar and pestle, a drastic colour change from blue to green was observed (Fig. S7). Importantly, the absolute fluorescence quantum yield was enhanced from 55 to 82% by grinding the crystalline sample into an amorphous state. Grinding of such crystalline solids induces a remarkable emission colour change from blue to green, a spectral emission shift up to 40 nm, as well as a noticeable 27% increase in emission quantum yield.

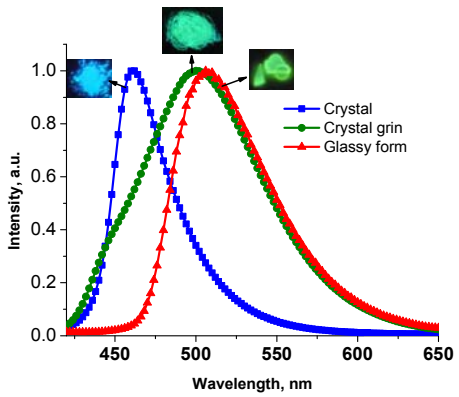

Fig. 3 Emission spectra of crystalline, amorphous, and glassy forms of *m*DCBP (insets: corresponding photograph under UV light)

This mechanochromism appears to be reversible as indicated by exposure of the ground sample to DCM solvent vapour for 3 min, with the emission colour reverting to that of the crystalline sample (Fig. 4). As indicated in Fig. 4, the emission maximum of *m*DCBP at 460 nm was red-shifted to 500 nm after grinding. This is likely due to an increase in intermolecular interactions resulting from the external pressure. As shown in Fig. S6, the powder X-ray diffraction (PXRD) pattern of *m*DCBP shows intense, sharp peaks for the crystalline form, with peak intensity drastically reduced after grinding. The intensity decrease indicates that the grinding process converted the crystalline *m*DCBP into an amorphous state. The observed small peaks in the PXRD pattern indicated that a small part of the crystalline sample remained after grinding, as can be seen from the emission spectra.

Interestingly, the green colour reverts to the blue colour after solvent diffusion. To demonstrate a practical application of *m*DCBP, 'NTHU' was written on the ground sample using a glass rod, with the letters showing high-contrast green emission. The letters were erased upon exposure to DCM solvent vapour for 3 min followed by writing 'TADF'. This reversibility of emission can be repeated many times without fatigue.

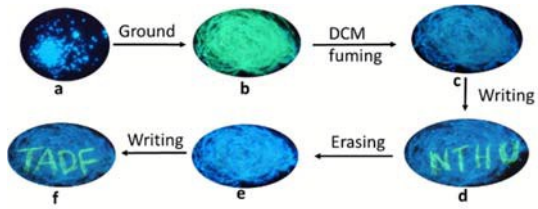

Fig. 4 Photograph of a) crystalline, b) after grinding, c) after solvent diffusion, d) writing of 'NTHU' e) letter erasing by solvent diffusion and f) writing of 'TADF' on the material.

Single-crystal XRD was used to understand the crystalline form molecular packing (structure shown in Fig. 5). The single-crystal analysis reveals that the molecules form dimers via intermolecular C=O---H interactions. This analysis also revealed that the pyridine ring interacts with a carbazole group of

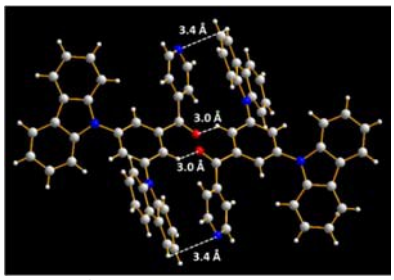

Fig. 5 Molecular packing of *m*DCBP.

Table 2. The EL performances of the device A-D using *m*DCBP as a dopant[a,b]

Device	V_d (V)	L (cd/m^2, V)	EQE (%, V)	CE (cd/A, V)	PE (lm/W, V)	λ_{max} (nm)	CIE (x,y), 8V
A	3.6	1870, 14.5	18.4, 3.0	34.0, 4.0	26.5, 4.0	474	(0.16;0.25)
B	3.2	3400, 12.0	17.9, 3.5	37.5, 3.5	33.5, 3.5	483	(0.16;0.30)
C	3.0	5010, 13.5	17.0, 3.5	38.0, 3.5	33.9, 3.5	488	(0.17;0.33)
D	2.8	8900, 18.0	14.7, 3.5	42.8, 3.5	38.2, 3.5	500	(0.22;0.44)

[a]Device configuration for A-D: ITO/NPB (40 nm)/*m*CP (10 nm)/DPEPO: *m*DCBP (10-30 wt%) (30 nm)/ PPT (5 nm)/ TmPyPb (60 nm)/LiF (1 nm)/Al (100 nm); [b]V_d, The operating voltage at a brightness of 1 cd/m^2; L, maximum luminance; EQE, maximum external quantum efficiency; CE, maximum current efficiency; PE, maximum power efficiency; and λ_{max}, the wavelength where the EL spectrum has the highest intensity.

another molecule. This interaction leads to blue emission, with this arrangement being destroyed by external pressure. The increase in intermolecular interaction then leads to red-shifted emission.

To investigate the electroluminescence properties of *m*DCBP, a multilayer OLEDs was fabricated using *m*DCBP doped films as the emitting layer (EML). The device structure and molecular structure used in the devices are shown in Fig. S8. Devices A-D is constructed with various concentration of *m*DCBP with the following device structure: ITO/NPB (40 nm)/*m*CP (10 nm)/DPEPO: *m*DCBP (X wt%) (30 nm)/PPT (5 nm)/TmPyPb (60 nm)/LiF (1 nm)/Al (100 nm), where x = 10, 15, 20, 30 and the corresponding devices are referred to as devices A, B, C and D, respectively. In this device, *N*,*N*′-bis(1-naphthyl)-*N*,*N*′-diphenyl-1,1′-biphenyl-4,4′-diamine (NPB) was used as a hole injection material, 1,3-bis(9-carbazolyl)benzene (*m*CP) as a hole-transporting material and also as an exciton blocker to prevent exciton diffusion to the NPB layer, while oxybis(2,1-phenylene))bis(diphenylphosphine oxide (DPEPO) was used as a host material, dibenzo[b,d]thiophene-2,8-diylbis(diphenylphosphine oxide) (PPT) was used as an exciton blockers and 1,3,5-tri(m-pyrid-3-yl-phenyl)benzene (TmPyPb) used as the electron transporting material.[9]

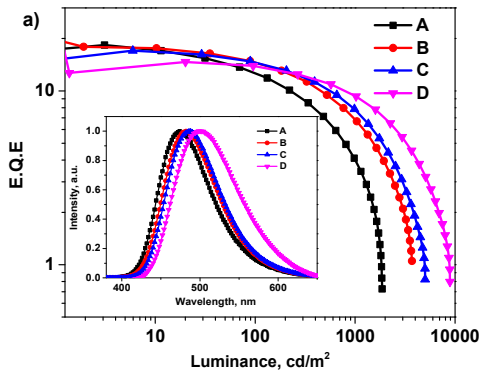

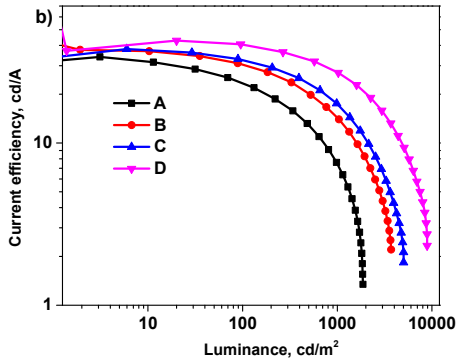

Fig. 6 a) External quantum efficiency of device A-D (inset: electroluminescent spectra of device A-D) and, b) Current efficiency vs luminance of device A-D.

Electroluminescence performance of the devices were shown in Fig.6, Fig.S9 and summarised in Table 2. It suggest that when the emitter concentration increased from 10-30% turn-on voltage of the devices are decreased 3.6 V to 2.8 V. EL spectra of the DPEPO:*m*DCBP devices in Fig. 6a show a gradual shift of the emission peak to long wavelength by increase of doping concentration because of intense intermolecular interaction. The colour coordinate of the devices (A-D) was shifted from (0.16, 0.25) at 10% doping to (0.22, 0.44) at 30% doping. However, the EQE of the device gradually increased from D to A, when the concentration of the emitter decreased from 30-10% (Table 2). Electroluminescence spectra of devices A-D remain relatively stable with increase in driving voltages, as shown in Fig. S10. Device A gave blue electroluminescence with a turn on voltage of 3.6 V and CIE (0.18, 0.25).[10] A maximum external quantum efficiency, current efficiency, and power efficiency of 18.4%, 34.0 cd/A, and 26.5 lm/W, respectively, was achieved. These efficiencies are comparable to those of blue phosphorescent OLEDs[10] and much higher than the conventional fluorescent devices. Device D showed a maximum luminance up to 8900 cd/m^2 at 18 V without any light out-coupling enhancement. The observed high device efficiencies suggest the existence of very efficient thermal up-conversion of

triplet excitons (T_1) to S_1 for this material. This result agrees well with the results of transient PL measurements that consisted of both fast and delayed fluorescent components (Fig. 2). Further, to confirm the TADF property, the transient electroluminescence decay was measured for device B at 3.5V. Fig. 7 shows that the delayed electroluminescence component lasts for several tens of microseconds. The result indicates that the EL efficiency is mostly contributed by the delayed fluorescence, supporting the existence of TADF process in the device.

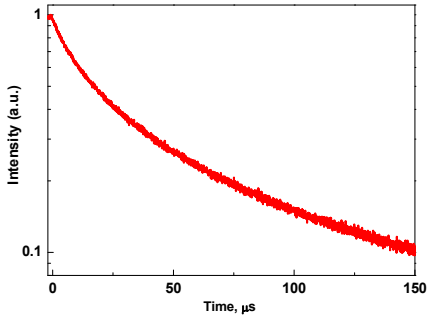

Fig. 7 Transient electroluminescence characteristics of device B measured at 3.5V.

In summary, we have successfully developed a TADF emitter, *m*DCBP, bearing a benzoylpyridine core as an electron-accepting unit and two *meta* carbazolyl groups as electron-donating units. This TADF emitter exhibits high-contrast reversible tunable emission and can be utilized in rewritable media. Blue and green OLEDs using *m*DCBP as the emitter achieved a maximum EQE value of 18.4 to 14.7%, a brightness reached up to 8900 cd/m^2. Therefore, this multifunctional TADF fluorescent emitter can be practically applied in OLED lighting panels and rewritable media.

We thank the Ministry of Science and Technology of Republic of China (MOST 103-2633-M-007-001) for support of this research and the National Center for High-Performance Computing (account number: u32chc04) of Taiwan for providing computing time.

Notes and references

1 a) A. Kishimura, T. Yamashita, K. Yamaguchi and T. Aida, *Nat. Mater.,* 2005, **4**, 546; b) H. B. Sun, S. J. Liu, W. P. Lin, K. Y. Zhang, W. Lv, X. Huang, F.W. Huo, H. R. Yang, G. Jenkins, Q. Zhao and W. Huang, *Nat. Commun.,* 2014, **5**, 3601; c) Z. Chi, X. Zhang, B. Xu, X. Zhou, C. Ma, Y Zhang, S. Liua and J. Xu, *Chem. Soc. Rev.*, 2012, **41**, 3878; d) S. S. Babu, V. K. Praveen and A. Ajayaghosh, *Chem. Rev.,* 2014, **114**, 1973; e) P. Rajamalli, P. Gandeepan, M.-J. Huang and C.-H. Cheng, *J. Mater. Chem. C,* 2015, **3**, 3329; f) A. Ajayaghosh, V. K. Praveen, C. Vijayakumar and S. J. George, *Angew. Chem. Int. Ed.,* 2007, **46**, 6260; g) T. Mutai, H. Satou and K. Araki, *Nature Mater.,* 2005, **4**, 685; h) D. Yan, J. Lu, J. Ma, M Wei, D. G. Evans and X. Duan, *Angew. Chem. Int. Ed.* 2011, **50**, 720.

2 a) R. Thirumalai, R. D. Mukhopadhyay, V. K. Praveen and A. Ajayaghosh, *Sci. Rep.,* 2015, DOI: 10.1038/srep09842; b) X. Hou, C. Ke, C. J. Bruns, P. R. McGonigal, R. B. Pettman and J. F. Stoddart, *Nat. Commun.,* DOI: 10.1038/ncomms7884; c) W. Lin, Q. Zhao, H. Sun, K. Y. Zhang, H. Yang, Q. Yu, X. Zhou, S. Guo, S. Liu and W. Huang, *Adv. Opt. Mater.,* 2015, **3**, 368.

3 a) Y. Dong, B. Xu, J. Zhang, X. Tan, L. Wang, J. Chen, H. Lv, S. Wen, B. Li, L. Ye, B. Zou and W. Tian, *Angew. Chem. Int. Ed.,* 2012, **51**, 10782; b) W. Z. Yuan, Y. Q. Tan, Y. Y. Gong, P. Lu, J. W. Y. Lam, X. Y. Shen, C. F. Feng, H. H. Y. Sung, Y.W. Lu, I. D. Williams, J. Z. Sun, Y. M. Zhang and B. Z. Tang, *Adv. Mater.,* 2013, **25**, 2837; c) L. Wang, K. Wang, B. Zou, K. Ye, H. Zhang and Y. Wang, *Adv. Mater.,* 2015, **27**, 2918; d) T. Butler, W. A. Morris, J. Samonina-Kosicka and C. L. Fraser, *Chem. Commun.*, 2015, **51**, 3359.

4 a) H. Uoyama, K. Goushi, K. Shizu, H. Nomura and C. Adachi, *Nature,* 2012, **492**, 234; b) T. Nakagawa, S. Y. Ku, K. T. Wong and C. Adachi, *Chem. Commun*., 2012, **48**, 9580; c) G. Méhes, H. Nomura, Q. Zhang, T. Nakagawa and C. Adachi, *Angew. Chem. Int. Ed*., 2012, **51**, 11311; d) H. Wang, L. Xie, Q. Peng, L. Meng, Y. Wang, Y. Yi and P. Wang, *Adv. Mater.,* 2014, **26**, 5198; e) X. Xiong, F. Song, J. Wang, Y. Zhang, Y. Xue, L. Sun, N. Jiang, P. Gao, L. Tian and X. Peng, *J. Am. Chem. Soc.,* 2014, **136**, 9590.

5 a) J. W. Sun, J.-H. Lee, C.-K. Moon, K.-H. Kim, H. Shin and J.-J. Kim, *Adv. Mater.,* 2014**, 26**, 5684; b) D. R. Lee, M. Kim, S. K. Jeon, S.-H. Hwang, C. W. Lee and J. Y. Lee, *Adv. Mater.,* 2015, DOI: 10.1002/adma.201502053; c) M. Kim, S. K. Jeon, S.-H. Hwang and J. Y. Lee, *Adv. Mater.,* 2015, **27**, 2515; d) Y. Tao, K. Yuan, T. Chen, P. Xu, H. Li, R. Chen, C. Zheng, L. Zhang and W. Huang, *Adv. Mater.,* 2014, **26**, 7931; e) W.-L. Tsai, M.-H. Huang, W.-K. Lee, Y.-J. Hsu, K.-C. Pan, Y.-H. Huang, H.-C. Ting, M. Sarma, Y.-Y. Ho, H.-C. Hu, C.-C. Chen, M.-T. Lee, K.-T. Wong and C.-C. Wu, *Chem. Commun.,* 2015, **51**, 13662; f) D. Zhang, L. Duan, C. Li , Y. Li , H. Li , D. Zhang and Y. Qiu, *Adv. Mater.* 2014, **26**, 5050; g) D. Zhang, L. Duan, D. Zhang and Y. Qiu, *J. Mater. Chem. C*, 2014, **2**, 8983.

6 M. N. Berberan-Santos and J. M. M. Garcia, *J. Am. Chem. Soc.,* 1996, **118**, 9391.

7 a) Q. Zhang, B. Li, S. Huang, H. Nomura, H. Tanaka and C. Adachi, *Nat. Photonics,* 2014, **8**, 326; b) S. Y. Lee, T. Yasuda, Y. S. Yang, Q. Zhang and C. Adachi, *Angew. Chem. Int. Ed.,* 2014, **53**, 6402; c) J. Lee, K. Shizu, H. Tanaka, H. Nomura, T. Yasuda and C. Adachi, *J. Mater. Chem. C*, 2013, **1**, 4599; d) H. Tanaka, K. Shizu, H. Miyazaki and C. Adachi, *Chem. Commun*., 2012, **48**, 11392; e) G. Méhes, H. Nomura, Q. Zhang, T. Nakagawa and C. Adachi, *Angew. Chem. Int. Ed.,* 2012, **51**, 11311; f) Y. J. Cho, S. K. Jeon, B. D. Chin, E. Yu and J. Y. Lee, *Angew. Chem.,* 2015, **127**, 5290.

8 C.-H. Shih, P. Rajamalli, C.-A. Wu, M.-J. Chiu, L.-K. Chu and C.-H. Cheng, *J. Mater. Chem. C*, 2015, **3**, 1491.

9 S.-J. Su, T. Chiba, T. Takeda and J. Kido, *Adv. Mater.,* 2008, **20**, 2125.

10 H.-H. Chou and C.-H. Cheng, *Adv. Mater.,* 2010, **22**, 2468.

A thermally activated delayed blue fluorescence emitter with reversible externally tunable emission

Pachaiyappan Rajamalli,[a] Natarajan Senthilkumar,[a] Parthasarathy Gandeepan,[a] Chen-Zheng Ren-Wu,[b] Hao-Wu Lin[b] and Chien-Hong Cheng*[a]

[a]Department of Chemistry, National Tsing Hua University, Hsinchu 30013, Taiwan.
E-mail: chcheng@mx.nthu.edu.tw

[b]Department of Materials Science and Engineering, National Tsing Hua University, Hsinchu 30013, Taiwan

A TADF material containing a benzoylpyridine core and two *meta* carbazolyl groups shows externally switchable emission in the solid states and a high external quantum efficiency of 18.4% when used as a blue dopant in OLED.